

Ionospheric Scintillations at L & C Bands

Yannick Béniguel^[1], J-P adam^[1], R. Prieto - Cerdeira^[2], B. Arbesser - Rastburg^[2]

IEEA, Courbevoie, France

ESA/ESTEC, Noordwijk, The Netherlands

beniguel@ieea.fr

jean-pierre.adam@club-internet.fr

roberto.prieto.cerdeira@esa.int

bertram@tec-ee.esa.int

Abstract— This paper addresses the problem of ionospheric scintillations at L and C bands. The results of a L band scintillation measurement campaign are presented. The receivers used during this campaign were located in the five regions of the globe allowing exhibiting the geographic similarities and discrepancies. Comparison with modeling has been done concurrently. The results presented for C band scintillations rely on cross checking the results with theoretical derivations.

I. INTRODUCTION

Transionospheric radio signals may experience amplitude and phase fluctuations due to the propagation through irregularities of the electron density inside ionosphere. These signal fluctuations may occur specially during equinoxes, after sunset and last a few hours. They are more intense in the periods of high solar activity. These fluctuations are responsible for signal degradation from the VHF up to the C band and may affect several applications as the navigation systems, the communications, the remote sensing and the earth observation systems.

The normalized standard deviation of the received intensity S_4 is used to classify the scintillation events: weak scintillations for $S_4 < 0.3$, medium scintillations for $0.3 < S_4 < 0.7$ and strong scintillations for $S_4 > 0.7$. The occurrence of strong scintillations events increases with the solar activity. Two regions of the globe are affected by such events: the equatorial regions (between -20° and $+20^\circ$ magnetic latitude) and the polar regions ($> 60^\circ$). The scintillations are more severe at the equator and the characteristics are different between the two regions.

In the frame of an ESA / ESTEC contract¹, we have conducted a measurement campaign for world coverage, including Africa and high latitudes (Sweden). This work involving several European teams is partly reported in this paper. The frequency of interest was the L band and we have used GPS receivers. Some of these receivers were regrouped in order to be able to derive the medium's correlation properties. That was the case in particular in Vietnam and in Africa. The data from the different locations has been stored with a common format to build a

data base. This data base has been analyzed and the results obtained have been compared with predictions given by two models.

A complementary study has been done for the C band². No data were found for C band scintillations. As C band scintillation corresponds to weak fluctuations, analytical derivation can be derived in that case, allowing cross checking the results provided by the GISM model [1] with analytic expressions when available.

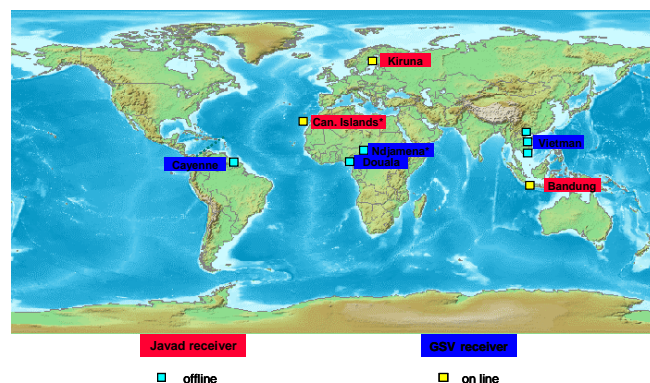


Figure 1 Receivers deployment

II. DATA BASE

L band scintillation data have been collected during years 2006 and 2007, consequently near the minimum of the solar cycle. Two types of monitors have been deployed in South America, Africa, Asia and in Europe at high latitudes, as shown on figure 1. The first type is a Legacy (from Javad or Topcon both identical in construction and operation mode). The second type is a GSV4004 based on a Novatel receiver [2]. Both types are operating at 50 Hz and provide additional channels to track geostationary satellites (when available). A data base has been constituted. Due to limited local support, it was not always possible to store the raw data files. In some locations the data were processed on line, stored, and sent back to Europe on a monthly basis. All the data have been used to derive the scintillation characteristics and improve scintillation models.

¹ ESTEC contract N° 19530 « Prediction of Ionospheric Scintillations », IEEA, DLR, GMV, CLS, Universities of Rennes & Brest

² ESTEC contract N° 21033 « Study and Modeling of Ionospheric Propagation Impairments at C-Band », IEEA, DLR, GMV, ICTP, Thales Alenia Space

In order to avoid considering data not representing ionosphere induced scintillations, we have discarded all data recorded with an elevation angle lower than 20° and a S4 level lower than 0.2. Assuming that these selected data show only scintillations of ionospheric origin, we get a reduced data set for subsequent analysis. The first observation is that only a very small part of the database is used in this study. The ionospheric scintillation was a rare event during the measurement campaign: only 0.2 % of the measured satellite/earth links were affected by unambiguous scintillations. However, despite the fact that it was solar minimum, high values of scintillation were recorded allowing deriving the statistical characteristics of scintillations.

III. DATA ANALYSIS

3.1 Pre-processed files

The pre-processed files contain the values of the scintillation indices of intensity (S4) and phase (sigma phi). Figure 2 below is typical of what was measured. It corresponds to data recorded in Vietnam and presents the intensity (S4) and phase (sigma phi) standard deviations of scintillations depending on the month. It shows in that case, that the maximum of scintillation activity occurs during equinoxes, on both sides of the equatorial anomaly.

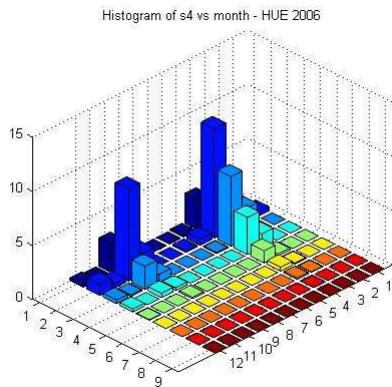


Figure 2: histogram of intensity and phase scintillations recorded in Vietnam. Horizontal axis: left, the value of S4 to be multiplied by 0.1; right the month number. Vertical axis: number (normalized) of events

This analysis has been made for all the receivers deployed with the same kind of results for all of them. However, although in all cases no scintillations were recorded in summer, the peak of the activity was not recorded in all places at equinoxes. This was the case in particular in Cayenne (French Guiana) where the maximum scintillation activity was in winter.

3.2 Raw data files

The scintillation spectra have been calculated from raw data files. To simplify the analysis, the raw data from all receivers were translated in Rinex format. In order to analyze all the downloaded raw data, the Power Spectral

Density (PSD) must be synthesized into a small number of parameters. The PSD is usually characterized by its strength at 1 Hz (T) and by its index of power law decay (p). On a log-log representation, these parameters are obtained by fitting a line to the data points using least squares. The frequency range for this line fit begins at 0.1 Hz, which is the cutoff frequency of the high-pass filter. This filter removes the low frequency parasitic fluctuations due in particular to the satellite motion on its orbit. In order to prevent this fit from extending down into the system noise which biases p towards lower values, the considered frequency range ends at 1 Hz.

This processing is applied to every 1 minute sample of the downloaded RINEX files considering the following criterions:

- No missing measurements (3000 points in a 1 minute sample)
- $S4 > 0.2$ to avoid multipath
- $\sigma_{phi} < 2$. to check the filter convergence

The following figure presents the histogram of the p index for the power PSD. This histogram is directly related to the probability density distribution of p. In that case, the distribution is centered on 2.8. Usually, p is considered to be in the range between 1 and 4. In addition, 2.5 is a commonly chosen value for p at equatorial latitudes. The observed distribution is compatible with this statement.

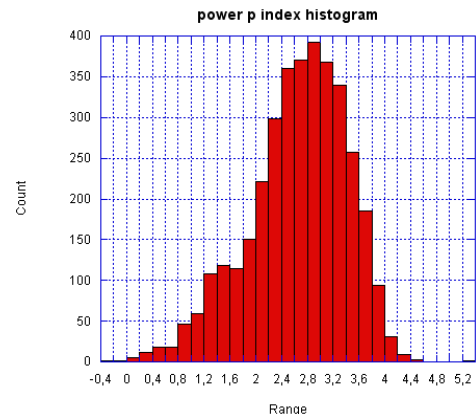


Figure 3: Intensity spectrum slope

IV. MODELING – MEASUREMENT COMPARISON

The measurements, selected according to our criterions, have been used for comparison with scintillation models. For each one of these selected data we have calculated the corresponding values given by the models: GISM developed under ESTEC contract and WBMOD [3]. WBMOD performs the calculation that we get scintillations at a given level with a desired percentile. This desired percentile is an input data that must be specified by the user. Depending on the value that the user puts on this figure, the S4 result may vary significantly. The results presented in this paper have been obtained with a percentile equal to 0.9.

GISM performs a calculation based on the propagation equations and gives a result with a confidence level. The user has not to indicate a probability. That one is a by-product of the calculation.

GISM accepts the Yuma files as an input. It has in addition an orbit generator. To perform the comparisons between the results of the two models, the orbit parameters were given to WBMOD. The two models were consequently executed with the same input data corresponding to the valid measurements. This was done for the 2 years 2006 and 2007.

Figure 4 shows a comparison of data measured in Vietnam and estimated using GISM and WBMOD models in year 2006. The 0.2 noise threshold in the measurements was due to multipath.

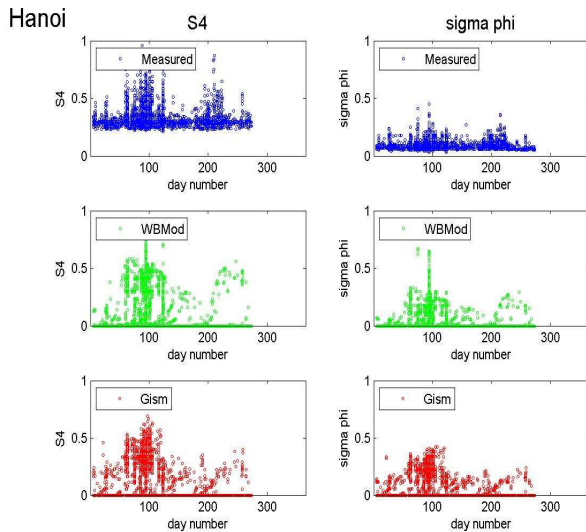


Figure 4: Comparison measurements - modeling in Hanoi depending on the day of year and on local time.

To analyse the latitudinal and longitudinal (or temporal) extent of the scintillations at the ionosphere level, we have approximated the ionosphere by a thin shell at 350 km of altitude. The Ionosphere Pierce Point (IPP) is defined as the intersection point of the satellite/earth link and this thin shell. For each valid sample, the recorded azimuth and elevation angle are used to compute the IPP latitude and longitude. The longitude is used to evaluate the local time at the IPP.

With an elevation mask of 20°, the latitudinal extent of the observed zone is about 14°. The temporal extent is set to 24 H, centered around midnight, since scintillations occur during night time. The observation zone is divided in a grid of 20 latitude points and 70 temporal points. For every station, all the IPPs observed during the measurement campaign are classed into the grid cells.

For each grid cell, the samples are counted and the mean value of the measured S4 and σ_{ϕ} are computed. These 3 parameters are good indicators of scintillation activity (only unambiguous scintillations measurements are taken into account). This kind of maps is the first step towards a cartography of the ionosphere irregularities.

The four stations located in Vietnam and Indonesia are located practically at the same longitude. The measurements recorded have been put on the same plot. It shows the global pattern. The horizontal stripes between -25° and -10° and between 4° and 10° correspond to the multipath in Hanoi and Bandung. The modeling results show a reasonable agreement.

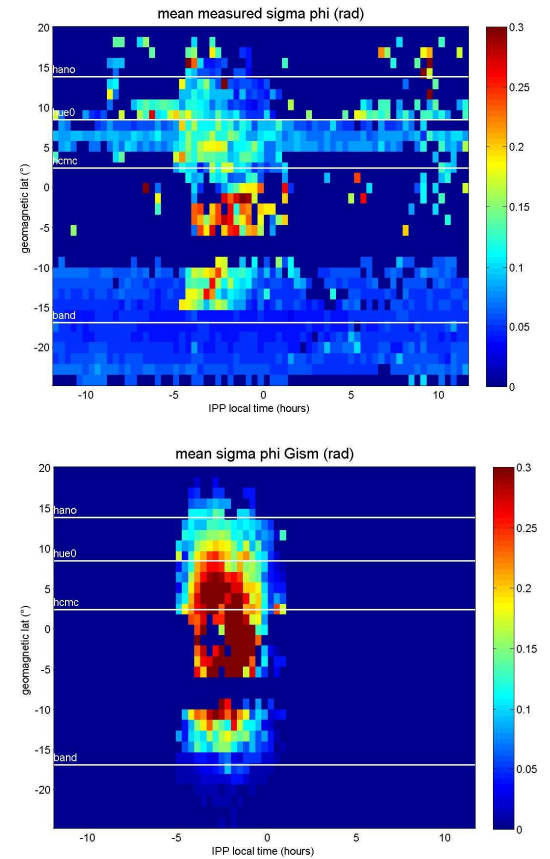


Figure 5: Comparisons model - measurements in Vietnam and Indonesia

GISM uses the NeQuick model [4] as a background to get the mean value of the electronic density. The NeQuick TEC maps reproduce quite well the equatorial anomaly with peaks on both sides of the magnetic equator. However the scintillations maps do not reproduce the anomaly. To conclude this, it is not obvious that a scintillation map should reproduce the same trends than a TEC map and this example shows the contrary. The same point has been addressed by [5] with similar observations.

V. UNDER SAMPLING AND IGS DATA

The IGS data are largely accessible all over the world but are recorded at 1 Hz which appears to be quite small as a sampling frequency for scintillations. The corresponding errors were quantified in this study

The phase PSD can be approximated by Tf^p . As a consequence, the phase standard deviation σ_{ϕ} is expressed as following, where f_c is the cutoff frequency :

$$\sigma_{phi}^2 = 2 \int_{f_c}^{\infty} PSD(f) df = 2 \int_{f_c}^{\infty} T f^{-p} df = 2T \left[\frac{f^{-p+1}}{-p+1} \right]_{f_c}^{\infty} = \frac{2T}{(p-1)f_c^{p-1}} \quad (\text{if } p > 1)$$

Figure 6 presents the effect of an under sampling for one typical example (satellite PRN 2, day 315, year 2006 at Cayenne (French Guiana)). The detrended 50 Hz raw data were sampled down to 1 Hz. As a consequence, the explored frequency range drops from 25 Hz to 0.5 Hz. In this example, it appears that the effect of the 1 Hz sampling is moderate.

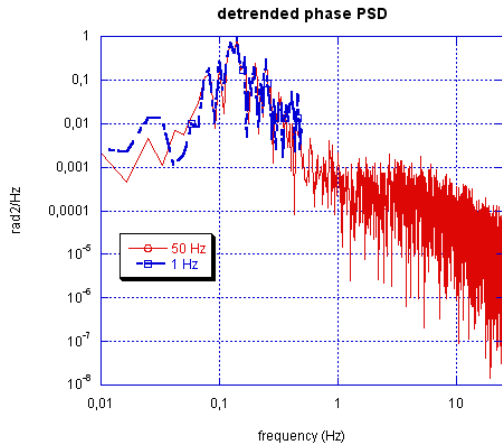


Figure 6: Undersampling at 1 Hz

In order to investigate the effect of the smaller frequency band, the integral used to compute σ_{phi} from the PSD is decomposed as follows:

$$\sigma_{phi}^2 = 2T \int_{0.1Hz}^{\infty} f^{-p} df \approx 2T \int_{0.1Hz}^{25Hz} f^{-p} df = 2T \left(\int_{0.1Hz}^{0.5Hz} f^{-p} df + \int_{0.5Hz}^{25Hz} f^{-p} df \right)$$

Setting p to 2.8, as corresponding to the measurements, we get:

$$\int_{0.1Hz}^{0.5Hz} f^{-2.8} df = 33 \quad \text{and} \quad \int_{0.5Hz}^{25Hz} f^{-2.8} df = 1.9$$

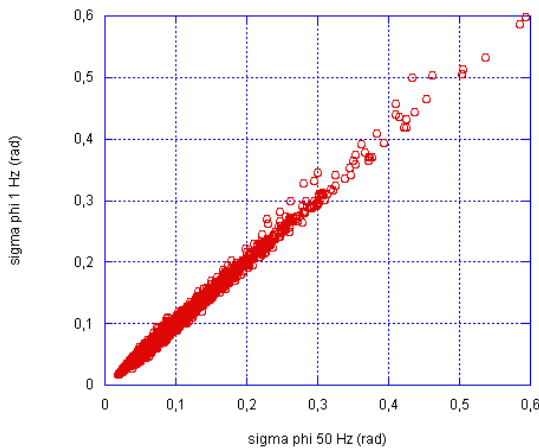


Figure 7: sigma phi calculated from 1 Hz data vs sigma phi calculated from 50 Hz data during 4 days at Cayenne

The part of the spectrum above 0.5 Hz is not significant. In other words, a sampling rate of 1 Hz seems to be sufficient to evaluate σ_{phi} in that case. In order to check this statement, every available 1 minute sample was down sampled to 1 Hz. The σ_{phi} computed over these 60 points samples are compared with the σ_{phi} computed over the full 3000 points samples. Figure 7 presents this comparison. It is observed that the 1 Hz σ_{phi} is a good estimation of the 50 Hz σ_{phi} .

The index chosen for the IGS data is the ROTI index [6]. It is a phase index deduced from the rate of change of the geometry after removing the mean variation using L1 and L2 frequencies. A day of severe scintillations at Cayenne has been selected for this comparison. The following plot shows the empirical ROTI scintillation index derived from the IGS 1 s data in Kourou. It compares quite well with the 1 mn S4 index recorded by the GSV receiver in Cayenne not reproduced here. This leaves the possibility using the IGS network to get some information on the scintillation activity. However a more systematic analysis should be made at higher solar activity to confirm these observations.

$$S4 \rightarrow [0.25-0.4], [0.4,0.55], [>0.55]$$

IGS : 1 sec at Kourou (ROTI Index per mn)

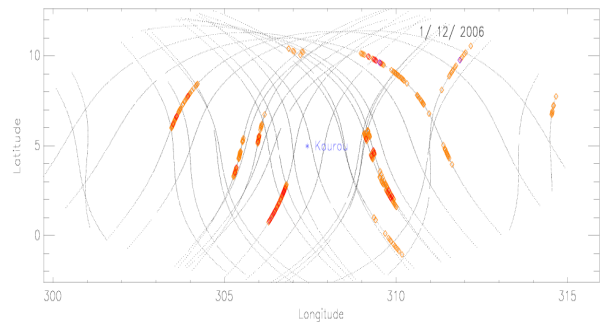


Figure 8: Scintillation index from IGS / Kourou for the 1st of Dec 2006 (the black lines are the projection of the GPS satellite pierce points at an altitude of 400 km)

VI. C BAND SCINTILLATIONS

No C band scintillation measurements data were found available. Consequently the assessment of GISM model was only possible by checking the results obtained by comparison with theoretical results when available.

The scintillations at C band correspond to weak scintillations even in the case of high solar activities. The GISM S4 peak values obtained are in the range of 0.2. In that case of low fluctuations, analytical calculations can be performed and this has been used to cross check the results obtained with GISM and consequently verify the adequacy of the model. The analytical calculations refer to the Rytov technique. The corresponding developments concern in particular the levels obtained, the probabilities and the correlation distances. It was shown in particular that in the case of low fluctuations, the probability of the Log

amplitude of the signal is Gaussian and that the correlation distances are large.

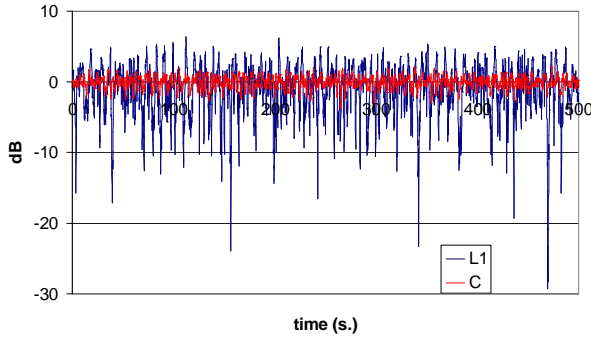


Figure 9: Intensity time series depending on the frequency

	L1	C band (5 GHz)	Ratio	Corr. coeff
S_4	0.65	0.19	3.42	0.2
σ_Φ	0.43	0.13	3.3	0.29

Table 1: S_4 and σ_Φ comparison for L1 and C bands

Figure 9 presents a typical example for intensity and phase scintillations. It shows the decrease with respect to the frequency.

Antenna aperture averaging

The scintillation S_4 and σ_Φ parameters are easily derived from the time/space series. Figure 10 presents the S_4 value as a function of the antenna size. A particular trans-ionospheric link with significant scintillation activity was considered. In order to check the behavior of the result at different scintillation levels, the solar flux number was modified in the GISM inputs. Both amplitude and phase scintillations are reduced by the antenna size. This decrease is faster for the amplitude. However, in order to check the result which was also derived analytically, the antenna size is very large and unrealistic. This result is a consequence of the signal coherence length which is very large at C band.

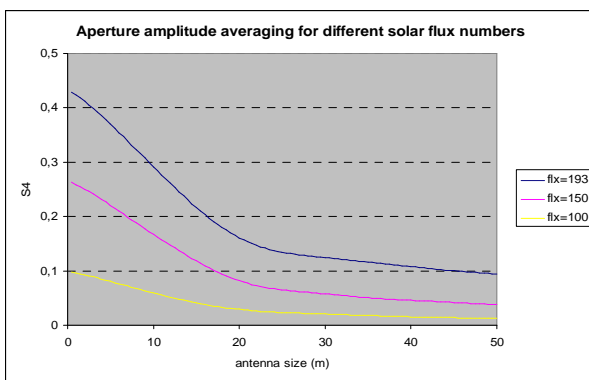


Figure 10: Intensity aperture averaging depending on the solar activity (flux number)

VII. CONCLUSION

The L band scintillation characteristics have been obtained from a data set including measurements from South America, Africa and Asia in years 2006 and 2007 corresponding to years close to the solar minimum. The expected behavior of scintillation occurrences has been found with some slight discrepancies between the different locations. In particular the maximum of scintillation occurrences occurs in winter in South America and at equinoxes in Vietnam. No scintillations were recorded at high latitudes and very few with the receiver located in the Canary Islands. At this location, the IPP maps produced show however a few points at very low latitudes corresponding consequently to the crest of the equatorial anomaly.

The latitude vs IPP maps which have been plotted allow obtaining a global view of the scintillation activity. It is quite easy to separate the different contributions: multipath, geostationary satellite contribution and scintillations. The comparison between the measurements and the models, although perfectible is not too bad and the analysis of the maps is of great interest.

As regards GNSS, one of the main sources of data unavailability that has been identified is the phenomenon of ionosphere scintillation. Such effect may induce loss of lock, cycle slips or excessive phase noise on ranging signals broadcast by Galileo satellites making them totally useless for accurate integrity determination. As indicated in the paper, the scintillations in C band will correspond to weak scintillations. The consideration of C band for future GNSS evolution can consequently be an effective way to improve the robustness of Galileo against scintillation.

REFERENCES

- [1] Béniguel Y., "GIM A Global Ionospheric Propagation Model for Scintillations of transmitted Signals", Radio Science, May-June 2002
- [2] Van Dierendonck A.J., GSV User manual, A.J. Systems, Los altos, Ca, USA
- [3] Secan, J.A., R.M. Bussey, E.J. Fremouw, "An improved model of equatorial scintillation", Radio Science, 30, 607 – 617, 1995
- [4] Leitinger, R., S. Radicella, B. Nava, „Electron density models for assessment studies – new developments“, Acta Geod. Geophys. Hung., 37, 183 - 193
- [5] Cervera M., R.M. Thomas "Latitudinal and temporal variations of equatorial ionospheric irregularities determined from GPS scintillation observations", Annals of Geophysics, 24, 3329 – 3341, 2006
- [6] J.J. Valette et al , "Observations of ionospheric perturbations on GPS signals at 50 Hz, 1 Hz and 0.03 Hz in South America and Indonesia", European Space Weather Week, Brussels, November 2007.